Controlled Release of Theophylline from Interpenetrating Blend Microspheres of Poly(vinyl alcohol) and Methyl Cellulose

Anita G. Sullad,[1] Lata S. Manjeshwar,[1] Tejraj M. Aminabhavi[2]

[1]*Department of Chemistry, Karnatak University, Dharwad 580 003, India*
[2]*CSIR Emeritus, Organic Coatings and Polymers Division, Indian Institute of Chemical Technology, Hyderabad 500007, India*

Received 22 June 2008; accepted 1 November 2008
DOI 10.1002/app.29625
Published online 18 December 2009 in Wiley InterScience (www.interscience.wiley.com).

ABSTRACT: Interpenetrating polymer network (IPN) microspheres of poly(vinyl alcohol) (PVA) and methylcellulose (MC) prepared by a water-in-oil emulsion method were crosslinked by glutaraldehyde and loaded with theophylline (THP), an antiasthmatic drug, with various ratios of PVA to MC. Microspheres were characterized with X-ray diffraction to determine the crystalline nature of the drug after encapsulation. Fourier transform infrared spectroscopy was used to assess the formation of the IPN structure and to confirm the absence of chemical interactions between the drug, polymer, and crosslinking agent. Differential scanning calorimetry confirmed the molecular-level distribution of THP in the polymer matrix, whereas scanning electron microscopy suggested the formation of clustered spherical particles. Zetasizer indicated that the particle sizes ranged from 4 to 57 μm. A THP encapsulation efficiency of up to 84% was achieved, as confirmed by ultraviolet spectrophotometry. Dynamic/equilibrium swelling experiments performed in pH 7.4 buffer media provided important information on drug diffusion characteristics. *In vitro* release studies performed in pH 1.2 and 7.4 buffer media indicated that the drug release depended on the extent of crosslinking as well as the amount of MC in the microspheres. Drug release was extended up to 3 h, and the results, as analyzed with an empirical equation, indicated non-Fickian transport for the release of THP. © 2009 Wiley Periodicals, Inc. J Appl Polym Sci 116: 1226–1235, 2010

Key words: biocompatibility; biomaterials; blends; crosslinking; differential scanning calorimetry (DSC)

INTRODUCTION

Controlled-release (CR) technology is a rapidly advancing science because of the development of innumerable types of polymers[1] and because it has several advantages over conventional dosage forms, including improved efficacy, reduced toxicity, improved patient compliance, and cost-effective therapeutic treatment. Such formulations have the ability to incorporate drugs without altering their integrity and maintain excellent *in vivo* compatibility. Among the different types of devices that have been developed, hydrogels are potential candidates for delivering bioactive molecules[2–4] because their open porous structure allows for the easy transport of the incorporated drug in a controlled manner. Self-regulated release from such hydrogels would enhance the release with the required sustained action.

Recent studies[5,6] on multicomponent polymers have provided convenient routes for modifying the properties of CR systems. Among such systems, considerable interest has been devoted to the development of interpenetrating polymer network (IPN) hydrogels[7–11] for the CR of drugs. An IPN is an intimate combination of two polymers, both in the same network, which can be obtained when at least one polymer is synthesized and/or crosslinked independently in the immediate vicinity of the other.[12] If only one component of the assembly is crosslinked, leaving the other in a linear form, the system is called a semi-IPN. Materials formed from IPNs share the properties of each network,[13] but the homopolymer cannot meet the divergent demands in terms of both properties and performance. Therefore, IPNs of two or three different polymers are better choices.[14]

Poly(vinyl alcohol) (PVA) is widely used in CR studies because of its hydrophilic and semicrystalline nature. Commercial-grade PVA is available in highly hydrolyzed grades (usually with a degree of hydrolysis > 98.5%) and partially hydrolyzed ones (with degrees of hydrolysis ranging from 80 to 98.5%). The degree of hydrolysis of PVA affects its chemical properties, solubility, and crystallizability; on the other hand, methylcellulose (MC) is a natural water-soluble polymer that can form reversible physical gels because of hydrophobic interactions when it is heated above room temperature.[15] Commercial-grade MC is produced by a chemical reaction in which cellulose is exposed to aqueous NaOH

Correspondence to: L. S. Manjeshwar (latamanjeshwar@yahoo.com).

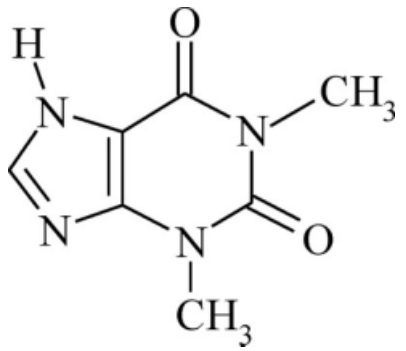

Figure 1 Chemical structure of THP.

and methyl chloride under mechanical mixing, with methylation occurring more rapidly in NaOH-rich and/or higher temperature regions. MC can be chemically crosslinked with dialdehyde in the presence of a strong acid to generate a hydrogel.[16–18]

In this research, we have developed IPN blend hydrogel microspheres of PVA and MC to encapsulate an antihistamine drug such as theophylline (THP), a water-soluble drug with a plasma half-time of 5–6 h (Fig. 1). Frequent doses are toxic, but the drug is effective for the treatment of asthma and pulmonary diseases.[19] It has been used as a model drug in earlier studies also.[20–24]

EXPERIMENTAL

Materials

THP was purchased from Loba Chemicals (Mumbai, India). PVA (weight-average molecular weight = 125,000) with a degree of hydrolysis of 86–89% and MC with a viscosity of 350–550 cPs were purchased from s.d. Fine Chemicals (Mumbai, India). An analytical-reagent-grade glutaraldehyde (GA) solution (25% v/v), petroleum ether, and liquid paraffin oil were all purchased from s.d. Fine Chemicals. Tween-80 was purchased from Loba Chemicals. The water used was a high-purity grade after double distillation and deionization.

Preparation of the IPN microspheres

Microspheres were prepared with different blend ratios of PVA to MC through the variation of the THP content and crosslinking agent. The microspheres that formed were characterized with Fourier transform infrared (FTIR) spectroscopy, scanning electron microscopy (SEM), X-ray diffraction (XRD), and differential scanning calorimetry (DSC) to investigate the chemical interaction of THP with the morphology of the prepared particles. Swelling experiments were carried out to evaluate the diffusion properties of THP through the microspheres. Release studies were performed in pH 1.2 and 7.4 buffer media at 37°C to find the optimum release patterns.

The emulsion crosslinking method was used in the preparation of IPN microspheres of PVA and MC.[11] Briefly, a 2 wt % PVA solution was prepared by dissolution in double-distilled deionized water and continuous stirring until a homogeneous solution was obtained. MC was then dispersed in a PVA solution and stirred overnight to obtain a homogeneous solution. THP was dissolved in the aforementioned polymer blend solution, and this solution was added slowly to light liquid paraffin (100 g, w/w) containing 1% (w/w) Tween-80 under constant stirring at 400 rpm for about 15 min. To this water-in-oil emulsion, GA as a crosslinking agent containing 0.1*N* HCl was added slowly, and the mixture was stirred for 3 h. Hardened microspheres were separated by filtration and washed with petroleum ether and water to remove the unreacted GA. The solid microspheres that were obtained were vacuum-dried at 40°C for 24 h and stored in a desiccator until further use. Totally, eight formulations were prepared according to the formulation codes assigned in Table I.

FTIR spectral measurements

FTIR spectral data were acquired with a Nicolet (Milwaukee, WI) Impact 410 instrument to confirm the formation of the IPN structure and also to find a possible chemical interaction of the drug with the IPN polymers. FTIR spectra of the placebo microspheres, drug-loaded microspheres, and pristine drug were obtained. Samples were ground with KBr, and pellets were obtained with a hydraulic pressure of 600 kg/cm^2. Spectral scanning was performed in the range of 4000–500 cm^{-1}.

DSC study

DSC (Rheometric Scientific, Surrey, United Kingdom) was performed on the THP-loaded microspheres,

TABLE I
Formulation Parameters of the Microspheres

Formulation code	PVA (% w/w)	MC (% w/w)	THP loading (%)	GA (mL)
F1	90	10	5	5
F2	90	10	10	5
F3	90	10	20	5
F4	80	20	10	5
F5	70	30	10	5
F6	90	10	10	2.5
F7	90	10	10	7.5
F8	100	00	10	5

TABLE II
Results for the Encapsulation Efficiency (EE), Mean Particle Size (d), Water Uptake (%), Empirical Parameters n and k, and Correlation Coefficient (r^2)

Formulation code[a]	EE from eq. (1) (%)	Water uptake from eq. (2) (%)	d (μm)	n from eq. (5)	k from eq. (5)	r^2
F1	57	209	6	0.34	0.336	0.975
F2	75	217	17	0.33	0.351	0.972
F3	83	284	27	0.31	0.388	0.943
F4	74	221	35	0.32	0.352	0.964
F5	70	231	57	0.32	0.374	0.961
F6	84	261	32	0.30	0.393	0.969
F7	55	171	4	0.37	0.300	0.977
F8	70	193	52	0.35	0.328	0.977

[a] Per detail in Table I.

placebo microspheres, and pristine THP. Samples were heated from 25 to 400°C at the rate of 10°C/min in a nitrogen atmosphere.

XRD studies

The crystallinity of THP after encapsulation was evaluated with XRD measurements recorded for the placebo microspheres, THP-loaded microspheres, and pristine THP with an X-ray diffractometer (X-Pert, Philips, United Kingdom). Scanning was done up to $2\theta = 50°$.

SEM studies

SEM images were taken with a JEOL (Japan) model JSM-840A instrument available at the Indian Institute of Science (Bangalore, India). Microspheres were sputtered with gold to make them conducting and placed on a copper stub. The thickness of the gold layer accomplished by gold sputtering was about 15 nm.

Particle size measurements

The particle sizes and size distributions were measured[25] with a Zetasizer (Model 3000HS, Malvern, Buntsford, United Kingdom). Particle size data for different formulations are included in Table II.

Drug content

The estimation of the drug concentration was done according to the method adopted by Rokhade et al.[24] Microspheres of a known weight (~ 10 mg) were ground to get the powder with an agate mortar, extracted with 50 mL of a pH 7.4 buffer solution, and sonicated for 30 min (UP 400s, Dr. Hielscher GmbH, Stahnsdorf, Germany). The solution was centrifuged (MR23i, Jouan, France) to remove polymeric debris and washed twice to extract the drug completely. The clear solution was analyzed with an ultraviolet spectrophotometer (Secomam, Anthelie, France) at the λ_{max} of 273 nm. The encapsulation efficiency (%) was calculated as follows:

$$\% \text{ Encapsulation efficiency} = \left(\frac{\text{Drug loading}}{\text{Theoretical drug loading}}\right) \times 100 \quad (1)$$

These data for various formulations along with other results are also given in Table II.

Swelling experiments

Equilibrium swelling of the drug-loaded microspheres was determined by the measurement of the extent of swelling of the microspheres in pH 7.4 buffer media. To ensure complete equilibration, samples were allowed to swell for 24 h, and excess surface-adhered liquid drops were removed by blotting with soft tissue paper. The swollen microspheres were weighed to an accuracy of ±0.01 mg on an electronic microbalance (AT120, Mettler, Greifensee, Switzerland). The hydrogel microspheres were dried in an oven at 60°C for 5 h until no change in the weight of the dried samples was observed. The equilibrium swelling (%) was calculated as follows:

$$\% \text{ Water uptake} = \left(\frac{\text{Weight of swollen microspheres} - \text{Weight of dry microspheres}}{\text{Weight of dry microspheres}}\right) \times 100 \quad (2)$$

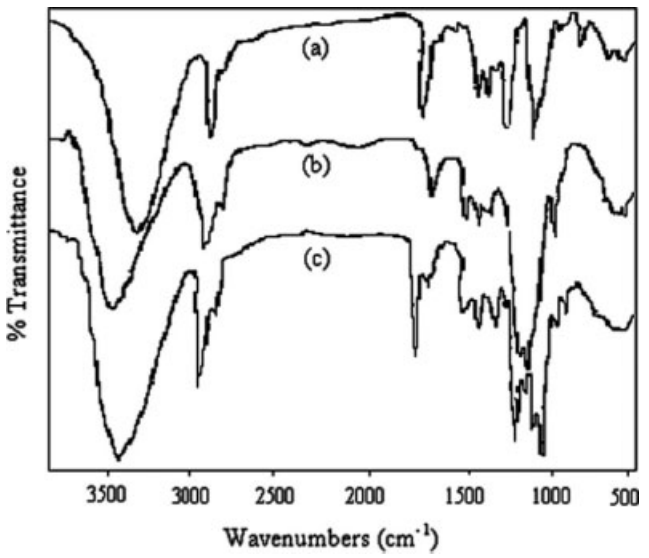

Figure 2 FTIR spectra of (a) PVA, (b) MC, and (c) placebo microspheres.

To understand the molecular transport of a drug-containing buffer solution into crosslinked microspheres, dynamic swelling data were collected with a microscopic technique.[26,27] The change in diameter of the microspheres in a buffer solution was monitored as a function of time. Experiments were performed in triplicate, but average values were considered for calculations and graphic display. The water uptake data (%) are also included in Table II.

In vitro release experiments

Drug release from IPN microspheres with different drug loadings (%), polymer blend compositions, and extents of crosslinking were investigated in 0.1*N* HCl for the initial 2 h, which was followed by a phosphate buffer at pH 7.4, until the completion of dissolution. These experiments were performed in triplicate with a tablet dissolution tester (LabIndia, Mumbai, India) equipped with eight baskets (glass jars) at the stirring speed of 100 rpm. A weighed quantity of each sample was placed in 500 mL of a dissolution medium maintained at 37°C. At regular time intervals, sample aliquots were withdrawn and analyzed with an ultraviolet spectrophotometer (Secomam) at the fixed maximum wavelength of 273 nm.

RESULTS AND DISCUSSION

FTIR spectral studies

FTIR spectra of plain PVA, plain MC, placebo microspheres, drug-loaded microspheres, and plain THP were taken to investigate the stability of THP after encapsulation. Figure 2 displays the FTIR spectra of plain PVA, plain MC, and placebo microspheres. In the case of PVA, a broad band observed at 3336 cm^{-1} can be attributed to O—H stretching vibrations. Two bands observed at 2937 and 2860 cm^{-1} represent the presence of C—H aliphatic stretching vibrations. MC has the characteristic band at 3450 cm^{-1} due to O—H stretching vibrations, whereas the two bands at 2928 and 2843 cm^{-1} can be attributed to C—H aliphatic stretching vibrations. In the case of placebo microspheres, all the characteristic bands of both PVA and MC can be observed in addition to a new band at 1018 cm^{-1} due to the presence of an acetal group formed by the reaction of GA with hydroxyl groups of MC and PVA. These data confirm the successful crosslinking of the PVA–MC IPN matrix with GA.

FTIR spectra were also used to confirm the chemical stability of THP in the IPN microspheres, as shown in Figure 3 for placebo microspheres, drug-loaded microspheres, and pure THP. In the case of THP, a broad band at 3434 cm^{-1} is due to N—H stretching vibrations. Bands at 3122, 3060, 2985, 2916, and 2826 cm^{-1} can be attributed to both aromatic and aliphatic C—H stretching vibrations. The band at 1715 cm^{-1} is characteristic of the imide stretching of the heterocyclic moiety (see Fig. 1). A sharp band at 1670 cm^{-1} is due to tertiary amide group stretching vibrations. The N—H bending vibration is shown at 1567 cm^{-1}, whereas the band at 1242 cm^{-1} can be attributed to C—N stretching vibrations. In the case of drug-loaded microspheres, all the bands that can be observed in THP also appear, indicating the chemical stability of THP even after encapsulation into the polymer matrix

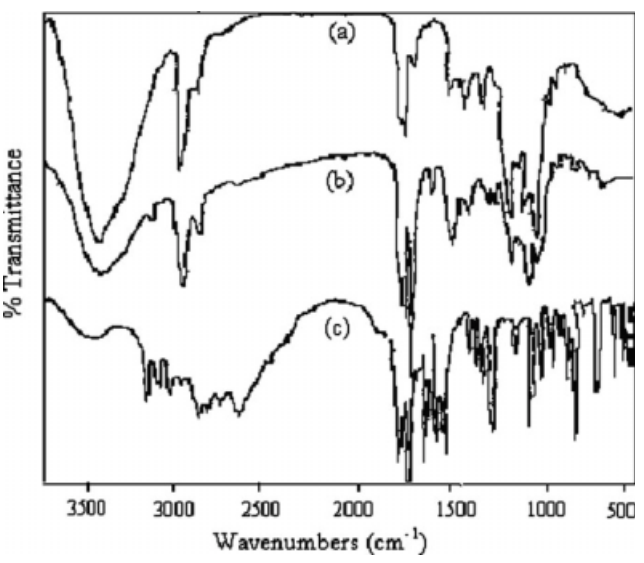

Figure 3 FTIR spectra of (a) placebo microspheres, (b) drug-loaded microspheres, and (c) pristine THP.

and the fact that no chemical interaction has occurred between the THP and IPN matrices.

DSC studies

DSC thermograms of placebo microspheres, drug-loaded microspheres, and pure THP are displayed in Figure 4. In the case of pristine THP, a sharp peak at 275°C can be observed, and it corresponds to the melting point of the drug. The thermogram of the placebo microspheres shows a broad peak at 90°C due to the endothermic transition of the polymer matrix. Similarly, the drug-loaded microspheres show the same pattern as that of the placebo, but no peaks can be observed at 275°C, and this indicates the amorphous nature even after the dispersion of the drug into the IPN matrix.

XRD studies

X-ray diffractograms of placebo microspheres, drug-loaded microspheres, and pristine THP are presented in Figure 5. The diffraction pattern of THP has characteristic intense peaks at $2\theta = 12.4^\circ$ that are identical to those of stable anhydrous THP crystal. This peak disappears for THP-loaded microspheres, and only peaks observed for the placebo polymer matrix can be seen. The XRD peak depends on the crystal size, but in this study, for all drug-loaded matrices, the characteristic peak of THP is overlapped by the noise of the polymer itself. Furthermore, even after encapsulation, THP is amorphous, so it is difficult to study its crystallinity at the detection limit of the crystal size. This clearly indicates that the drug is dispersed molecularly in the polymer matrix, and so no crystals were found in the drug-loaded matrices.

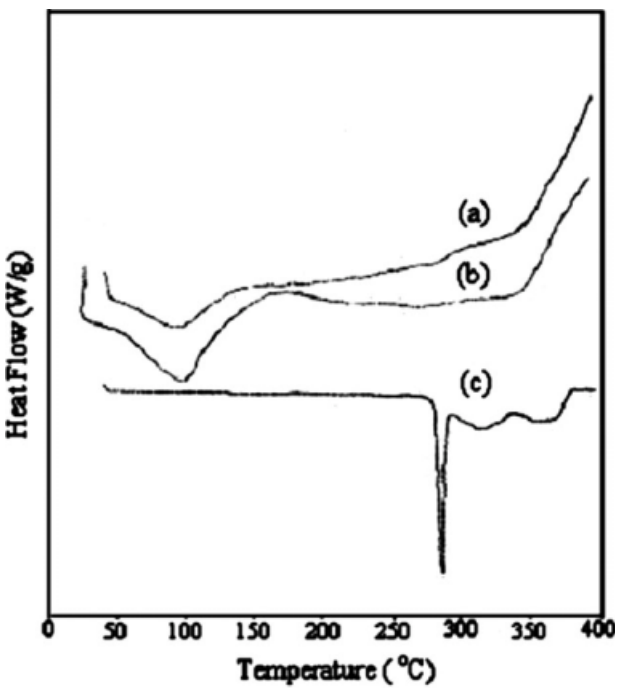

Figure 4 DSC thermograms of (a) placebo microspheres, (b) drug-loaded microspheres, and (c) pristine THP.

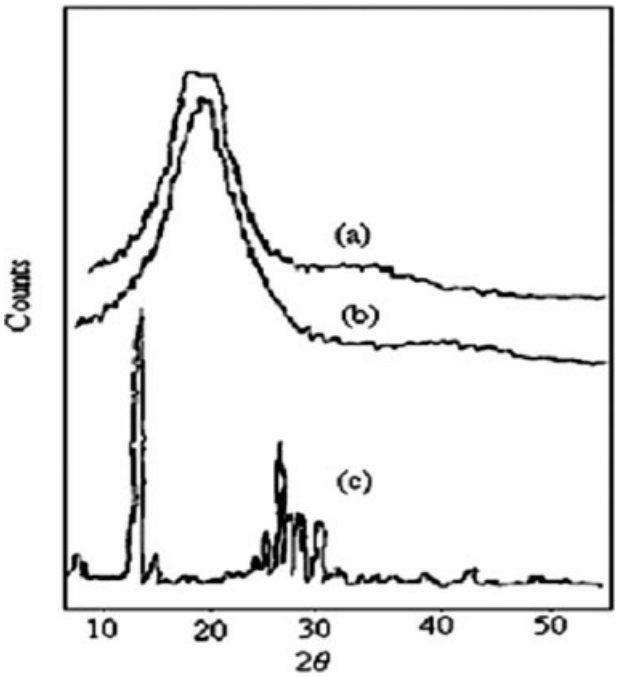

Figure 5 XRD spectra of (a) placebo microspheres, (b) drug-loaded microspheres, and (c) pristine THP.

SEM studies

SEM images of the microspheres taken at magnifications of 2000 and 750× are shown in Figures 6

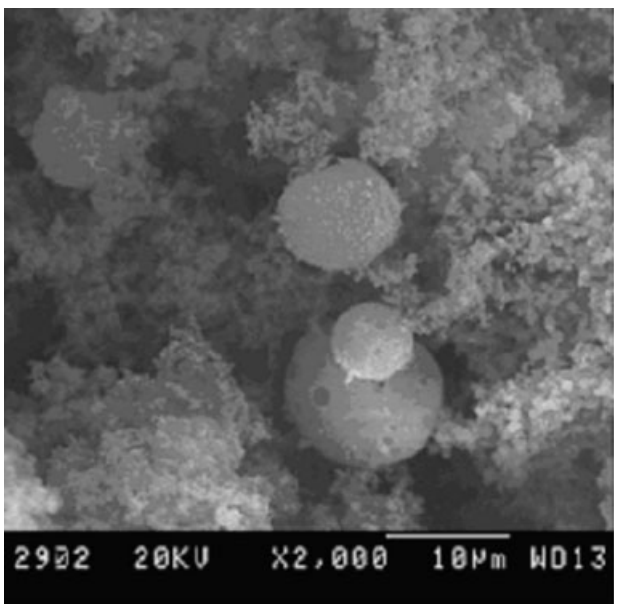

Figure 6 Scanning electron micrograph of PVA-MC blend microspheres.

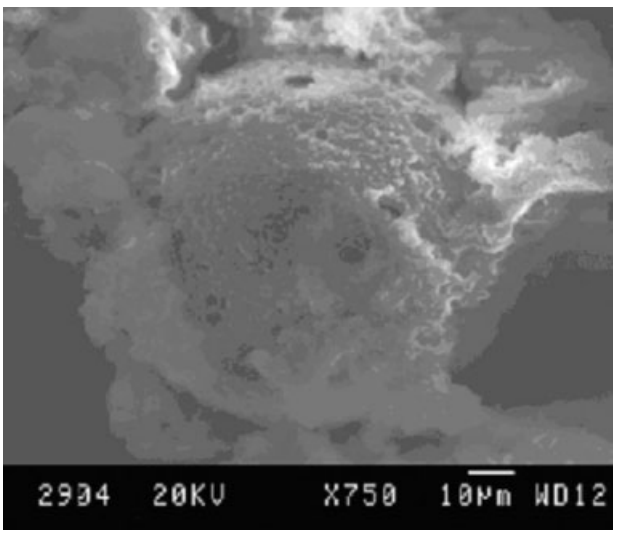

Figure 7 Scanning electron micrograph of a single microsphere.

and 7, respectively. Even though the microspheres seem to be spherical in nature, one can observe particle agglomeration with somewhat rough surfaces. Also, polymeric debris seen around the particles is probably due to the method of particle production (i.e., simultaneous particle production and IPN blend matrix formation) as well as the presence of more amorphous MC in the IPN matrix. Microspheres produced by blending with different compositions of PVA and MC did not show any systematic morphological effect on their surfaces.

Particle size

The results for the mean particle size are presented in Table II, whereas the size distribution curve for one typical formulation (F4) containing 20 wt % MC, 10 wt % drug, and 5 mL of GA is displayed in Figure 8. Similar to the results for the encapsulation efficiency and water uptake (%), the size of the microspheres depends on the amount of drug in the IPN matrix, the MC content (%), and the extent of crosslinking of the matrix. Microspheres range between the sizes of 4 and 57 μm, but with an increasing amount of MC in the blend matrix, the size of the microspheres increased from 17 to 57 μm; this dependence is typically seen with 10 wt % THP-loaded microspheres. Particle size measurements using a Zetasizer cannot offer the exact shape of the particles produced, but their exact size measurement is possible. With an increasing amount of THP in the matrices, the size of the particles also increased. For formulations containing 10 wt % MC with different amounts of THP, the particle size also increased from 6 to 27 μm (see Table II), probably because THP occupied the available free volume spaces of the blend microspheres.[27] Note that the particle size decreased with increasing crosslink density because with increasing GA content of the matrix, shrinkage of the matrix occurred, thereby reducing the size of the microspheres.[27,28] For instance, as the amount of GA increased from 2.5 to 7.5 mL, the particle size decreased from 32 to 4 μm.

Encapsulation efficiency

For any new formulation to be used successfully, it is necessary to achieve a high encapsulation efficiency of the drug. As reported in our previous studies,[7,24] encapsulation efficiency values are dependent on process variables such as the drug–polymer ratio, blend composition, and extent of the crosslinking agent. The formulations displayed in Table II show these effects. For instance, in the case of formulations F1, F2, and F3, which contained 90 wt % PVA, 10 wt % MC, and 5 mL of GA, the encapsulation efficiency values increased systematically from 57 to 75 and 83% with increasing THP loadings, but when the blend compositions were altered (i.e., 80 and 70 wt % PVA with 20 and 30 wt % MC) and the THP loading (10 wt %) and amount of GA (5 mL) were kept constant, the encapsulation efficiency values decreased slightly from 74 to 70 for formulations F4 and F5, respectively. On the other hand, for 90 wt % PVA with 10 wt % MC blends (i.e., F6 and F7) with a constant THP loading of 10 wt % and an amount of GA varying from 2.5 to 7.5

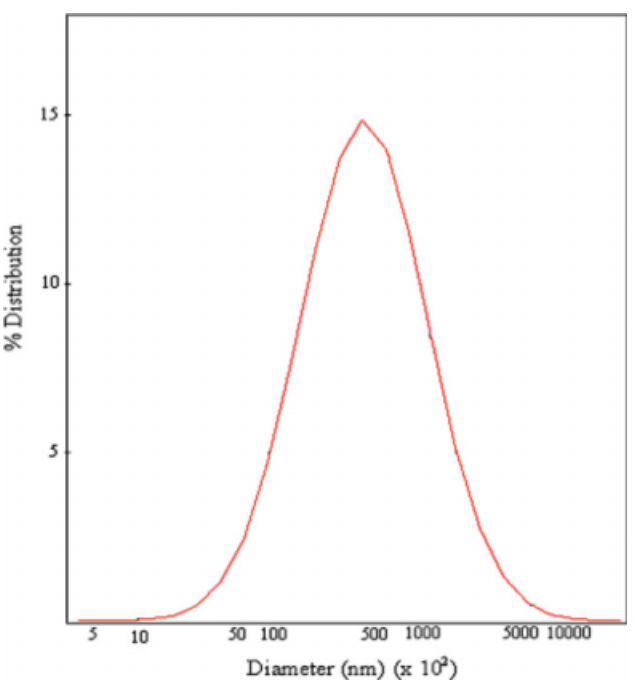

Figure 8 Particle size distribution of PVA–MC blend (F4) microspheres. [Color figure can be viewed in the online issue, which is available at www.interscience.wiley.com.]

mL, we observed a decrease in the encapsulation efficiency values from 84 to 55%, which indicated the more rigid nature of the IPN matrix with a higher amount of GA (viz. 7.5 mL) due to the higher crosslink density. Comparatively, a pure PVA matrix with 10 wt % THP and 5 mL of GA showed an encapsulation efficiency of 70%. It is thus clear that encapsulation efficiency values are affected greatly by the process variables during formulation steps, as reported previously.[24]

Swelling (% uptake) studies

Drug release rates are also influenced by equilibrium swelling of the crosslinked microspheres.[29] The equilibrium swelling (%) data of the crosslinked microspheres presented in Table II indicate that, as the amount of GA in the matrices increased from 2.5 to 7.5 mL, equilibrium swelling decreased significantly from 261 to 171%. This type of reduction in swelling is due to the formation of a rigid IPN matrix at a higher crosslink density. Note that formulations containing higher amounts of MC exhibited higher swelling rates. For instance, formulation F5 (30 wt % MC) exhibited higher swelling than F4 (20 wt % MC) because of the more hydrophilic nature of MC versus PVA; this allowed the matrix to absorb a greater amount of water than PVA.

To understand more quantitatively the extent of dynamic swelling, we monitored the diameter changes of the microspheres as a function of time using an optical microscope. Figure 9 displays the plot of normalized diameter D_t/D_o (where D_o is the original diameter of the microsphere and D_t is the diameter of the swollen particles at time t) as a function of time for matrices F2, F6, and F7 with different extents of crosslinking. D_t/D_o of the microspheres decreased with an increasing amount of GA in the matrix because of the rigid nature acquired with a greater amount of GA. Figure 10 displays a plot of D_t/D_o versus t for formulations F2, F4, and F5 (different polymer compositions) of the blend matrix and for the plain PVA matrix (F8). D_t/D_o increased with an increasing amount of MC because of the hydrophilic nature of MC, which enhanced the water uptake capacity of the blend matrix in comparison with the plain PVA. The results of the equilibrium swelling diameter, D_∞, normalized to original diameter, D_o, are presented in Table III.

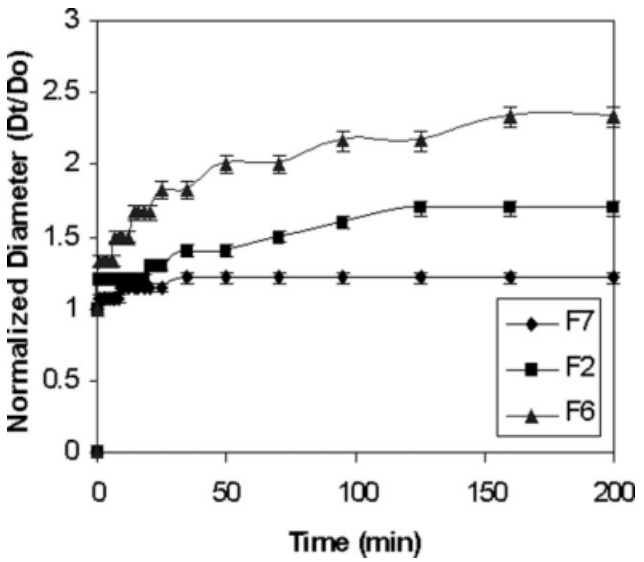

Figure 9 Plot of D_t/D_o versus time t demonstrating the effect of crosslinking for formulations F7 (7.5 mL of GA), F2 (5 mL of GA), and F6 (2.5 mL of GA).

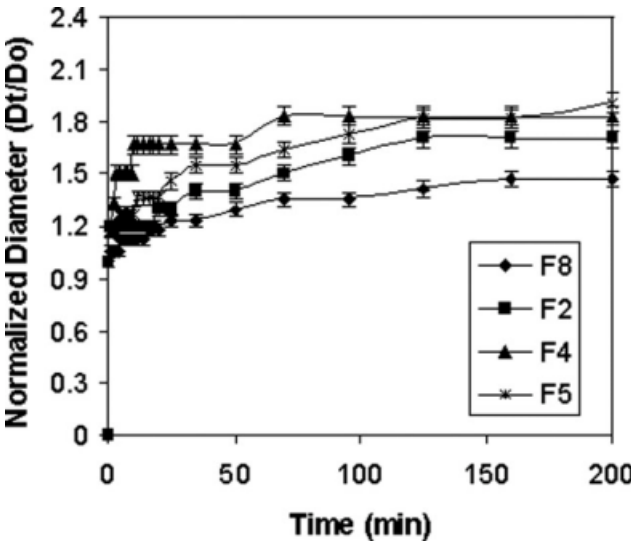

Figure 10 Plot of D_t/D_o versus time t demonstrating the effect of the polymer blend ratio for formulations F8 (pure PVA), F2 (10 wt % MC), F4 (20 wt % MC), and F5 (30 wt % MC).

Further efforts have been made to estimate the dimensional changes of the microspheres during matrix swelling [in terms of the volume change as a function of time (ΔV_t) with respect to the initial volume (V_o) of the matrix]. Diffusion coefficient (D_v) values of water were computed with eq. (3)[30]:

TABLE III
Transport Results for the Drug-Loaded Microspheres at 37°C

Formulation code	D_∞/D_o	D_v ($\times 10^{+6}$ cm^2/s)	u (10^{+3} cm/s)
F1	1.60	0.33	5.38
F2	1.70	0.35	6.42
F3	1.80	0.86	13.15
F4	1.83	1.40	6.79
F5	1.91	1.45	11.38
F6	2.33	1.17	12.20
F7	1.21	0.18	1.93
F8	1.47	0.27	5.08

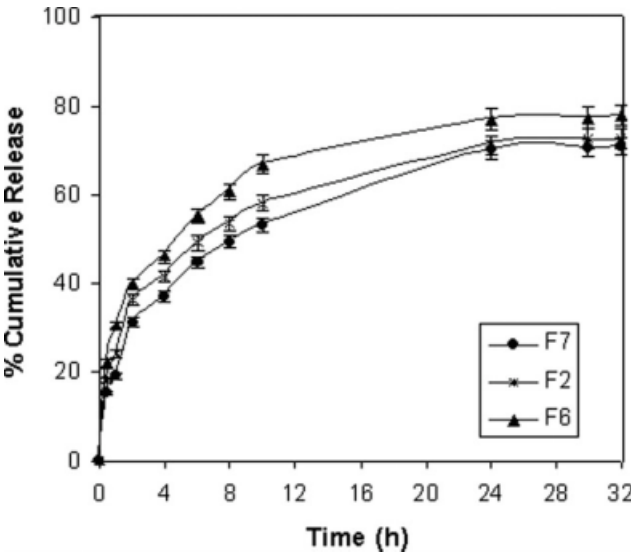

Figure 11 Effect of crosslinking on the *in vitro* release for formulations F7 (7.5 mL), F2 (5 mL), and F6 (2.5 mL) at 37°C.

$$D_v = [(1.773 \times \text{Slope})V_o D_o/4V]^2 \quad (3)$$

The values of D_v were computed from the slopes of the initial linear plots of $\Delta V_t/V_o$ versus $t^{.1/2}$ These results are also included in Table III.

Solvent migration through polymeric matrices is also important for understanding drug diffusion characteristics. To understand this effect, we have computed the solvent front velocity (u) of the advancing boundary[31] in the microspheres using eq. (4):

$$u = \left(\frac{dv}{dt}\right)\frac{1}{A} \quad (4)$$

where dv/dt represents the change in volume of the microspheres per unit of time and A is the total area of the microsphere calculated with consideration of its spherical geometry [$V = (4/3)\pi r^3$]. The results of u are also included in Table III. Note that D_v and u decreased with increasing crosslink density of the matrix; that is, with the amount of GA increasing from 2.5 to 7.5 mL, a considerable decrease in D_v was observed from 1.17×10^{-6} to 0.18×10^{-6} cm^2/s. Similarly, a decrease in u occurred from 12.2×10^{-3} to 1.9×10^{-3} cm/s. Thus, with greater amounts of MC, D_v and u values were higher because the overall PVA–MC blend matrix became more hydrophilic than PVA alone. The molecular transport of drug-containing liquid media through the microspheres is thus found to be dependent on the extent of crosslinking. With lower amounts of GA, the blend network is somewhat loose with a high hydrodynamic free volume to accommodate more solvent molecules, and this causes it to swell. In the case of hydrogels of the type used here, the transport of a drug-loaded solution depends on the extent of the hydrodynamic free volume, which facilitates the drug solution to permeate through the membrane barrier.

In vitro release studies

In vitro release experiments with THP in IPN microspheres of PVA and MC were performed under gastric (pH 1.2) and intestinal (pH 7.2) conditions. The average data of the cumulative release (%) versus time plots for drug-loaded microspheres in the case of formulations F2, F6, and F7 are compared in Figure 11 to understand the extent of crosslinking in *in vitro* release profiles. Formulation F2 exhibited higher release than F7, and similarly, F6 exhibited higher release than either F2 or F7. Note that F7 had a greater amount of GA (7.5 mL) than F2 or F6, and this made it more rigid than F2 or F6. This resulted in a decreased cumulative release (%) of THP. In fact, F6, that is, the matrix with a smaller amount of GA (2.5 mL), had higher release rates because of the lesser rigidity of the matrix. In all cases (F2, F6, and F7), the release trends followed identical patterns, and the release was extended up to 32 h. Figure 12 displays the effect of the polymer blend composition as envisaged in formulations F2, F4, and F5; these data are also compared with formulation F8, which was 100% PVA. The cumulative release (%) was higher in case of the F5 versus F4 because of the higher MC content of the blend polymer matrix. Similarly, F4 showed a higher release rate than F2. In all cases, maximum release of THP occurred in 24 h, which was extended up to 32 h.

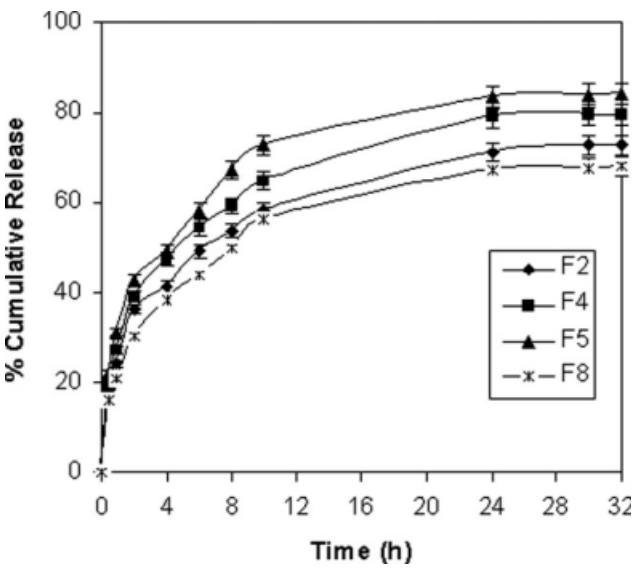

Figure 12 Effect of the polymer blend ratio on the *in vitro* release for formulations F2 (10 wt % MC), F4 (20 wt % MC), and F5 (30 wt % MC) at 37°C.

The effect of the drug loading (%) on *in vitro* release for formulations F1, F2, and F3 is displayed in Figure 13, which shows that formulation F3 had a higher release rate than F2. Similarly, F2 had a higher release rate than F1. This clearly depicts the dependence of THP release on the amount of drug loaded in the matrices; that is, release was higher for those formulations having a greater amount of the drug and vice versa. However, during the first 2 h of the drug release experiments, dissolution was performed in 0.1*N* HCl; we observed burst release for all formulations, and release was extended up to 32 h. This is clear evidence that when THP-loaded formulations are being developed, it is important to simultaneously consider appropriate variations in the process parameters during the formulation stage to develop a final product that yields optimal release profiles. Nearly 80% of the drug was released from the developed formulations.

In Figures 11–13, the error bars indicate a maximum standard deviation of 3% from the average curves. These data were computed from the statistical average data package employed at the 95% confidence limit.

To establish the relationship between the drug release and molecular transport mechanism, cumulative release data were fitted to an empirical equation[29]:

$$M_t/M_\infty = kt^n \quad (5)$$

where M_t/M_∞ represents the fractional drug release at time t, k is a parameter characteristic of the drug–polymer system, and n is an empirical parameter characterizing the release mechanism. Using the least-squares procedure at the 95% confidence limit, we estimated the values of n and k for all eight formulations, and these data along with the correlation coefficients are included in Table II. For $n = 0.5$, the drug diffuses and is released from the polymer matrix according to Fickian diffusion. For $n > 0.5$, anomalous or non-Fickian transport exists. For $n = 1$, non-Fickian transport, which is more commonly called case II transport, is operative. When the values of n vary between 0.5 and 1.0, transport is classified as anomalous.[32]

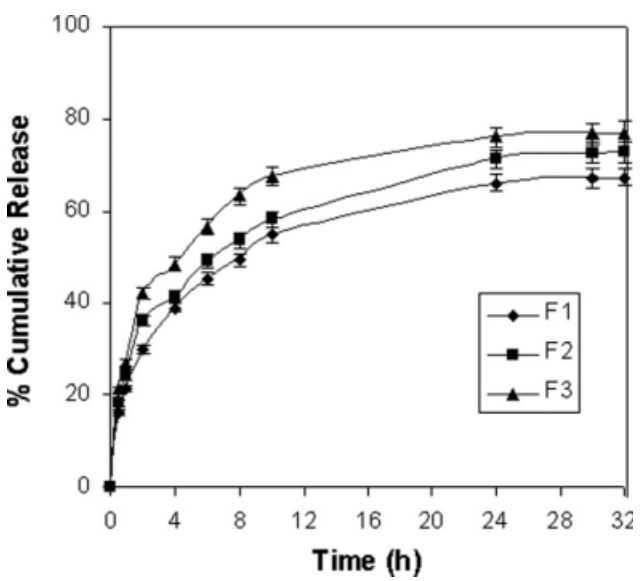

Figure 13 Effect of the drug loading (%) on the *in vitro* release for formulations F1 (5 wt %), F2 (10 wt %), and F3 (20 wt %).

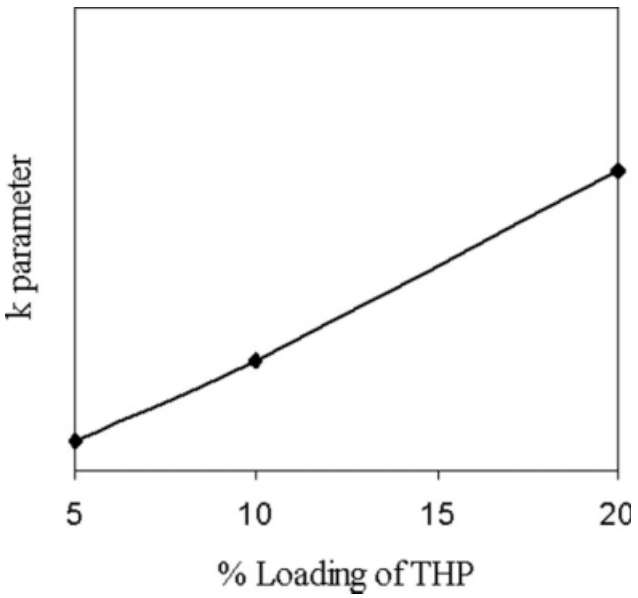

Figure 14 Effect of the loading (%) of THP on parameter k calculated from eq. (5).

The values of n and k are dependent on the extent of crosslinking and the loading (%) of THP. A plot of k values versus the THP loading (%) is shown in Figure 14, which indicates that k increases with an increasing loading of THP, but decreases with increasing crosslinking of the PVA–MC matrix. The n values for microspheres crosslinked with 2.5 mL of GA were smaller than those found for microspheres crosslinked with 5 or 7.5 mL of GA, probably because of the loose crosslinking of the network, which led to higher swelling. The values of n were higher for microspheres that were crosslinked with 7.5 mL of GA because of the formation of the rigid IPN matrix. In any case, the n values for the microspheres ranged from 0.3 to 0.37, indicating that THP release from the microspheres followed non-Fickian trends.

CONCLUSIONS

The results of this work have demonstrated the feasibility of preparing interpenetrating blend microspheres of PVA with MC in the size range of 4–57

μm, which have been found to be effective in producing formulations with extended release of THP (up to 32 h). It was observed that drug encapsulation in the microspheres was dependent on the type of blend matrix, the extent of crosslinking, and the drug loading. A burst effect was observed with a cumulative release of 15–35% because of the immediate release of THP from the matrix materials, which was extended up to 32 h, offering a cumulative release of 80%. The cumulative release rates (%) were dependent on the nature of the delivery matrix. A maximum of 84% encapsulation efficiency was observed, depending on the nature of the matrix. Diffusion parameters were computed, and the kinetics of release profiles were established. The computation of parameters from the empirical equation suggested a non-Fickian nature of the transport mechanism.

The authors (Miss. A. G. Sullad and Prof. L. S. Manjeshwar) are thankful to University Grants Commission (UGC), New Delhi, India for financial support in the form of a fellowship. Prof. T. M. Aminabhavi thanks CSIR for award of Emeritus Scientist.

References

1. Agnihotri, S. A.; Mallikarjuna, N. N.; Aminabhavi, T. M. J Controlled Release 2004, 100, 5.
2. Itokazu, M.; Yamemoto, K.; Yang, W. Y.; Aoki, T.; Kato, N.; Watanabe, K. Infection 1997, 25, 359.
3. Kawaguchi, H. Prog Polym Sci 2000, 25, 1171.
4. Yao, K. D.; Peng, T.; Feng, H. B.; He, Y. Y. J Polym Sci Part A: Polym Chem 1994, 32, 1213.
5. Ekici, S.; Saraydin, D. Drug Delivery 2004, 11, 381.
6. Verestiue, L.; Ivanov, C.; Barbu, E.; Tsiboukhis, J. Int J Pharm 2004, 269, 185.
7. Agnihotri, S. A.; Aminabhavi, T. M. Drug Dev Ind Pharm 2005, 31, 491.
8. Kurkuri, M. D.; Aminabhavi, T. M. J Controlled Release 2004, 96, 9.
9. Kulkarni, A. R.; Soppimath, K. S.; Aminabhavi, T. M. J Pharm Biopharm 2001, 51, 127.
10. Soppimath, K. S.; Kulkarni, A. R.; Aminabhavi, T. M. J Biomater Sci Polym Ed 2000, 11, 27.
11. Rokhade, A. P.; Agnihotri, S. A.; Patil, S. A.; Mallikarjuna, N. N.; Kulkarni, P. V.; Aminabhavi, T. M. Carbohydr Polym 2006, 65, 243.
12. Agnihotri, S. A.; Aminabhavi, T. M. Int J Pharm 2006, 324, 103.
13. Kosmala, J. D.; Henthorn, D. B.; Peppas, L. B. Biomaterials 2000, 21, 2019.
14. Changez, M.; Burugapalli, K.; Koul, V.; Choudhary, V. Biomaterials 2003, 24, 527.
15. Haque, A.; Morris, E. R. Carbohydr Polym 1993, 22, 161.
16. Gimenez, V.; Reina, J. A.; Cadiz, V. Polymer 1999, 40, 2759.
17. Horkay, F.; Zrinyi, M. Macromolecules 1982, 15, 1306.
18. Tomita, E.; Ikeda, Y. J Polym Sci Part A: Polym Chem 1997, 35, 3553.
19. Yu, Z.; Schwartz, J. B.; Sugita, E. T. Biopharm Drug Dispos 1996, 17, 259.
20. Antal, I.; Zelkó, R.; Roczey, N.; Plachy, J.; Rácz, I. Int J Pharm 1997, 155, 83.
21. Coviello, T.; Grassi, M.; Lapasin, R.; Marino, A.; Alhaique, F. Biomaterials 2003, 24, 2789.
22. Katime, I.; Novoa, R.; Zuluaga, F. Eur Polym J 2001, 37, 1465.
23. Shozo, M.; Wataru, K.; David, A. J Controlled Release 2000, 67, 275.
24. Rokhade, A. P.; Shelke, N. B.; Patil, S. A.; Aminabhavi, T. M. Carbohydr Polym 2007, 69, 678.
25. Agnihotri, S. A.; Aminabhavi, T. M. J Microencapsul 2004, 21, 709.
26. Robert, C. C. R.; Buri, P. A.; Peppas, N. A. J Appl Polym Sci 1985, 30, 301.
27. Soppimath, K. S.; Kulkarni, A. R.; Aminabhavi, T. M. Eur J Pharm Biopharm 2002, 53, 87.
28. Korsmeyer, R. C.; Peppas, N. A. J Membr Sci 1981, 9, 211.
29. Ritger, P. L.; Peppas, N. A. J Controlled Release 1987, 5, 37.
30. Harogoppad, S. B.; Aminabhavi, T. M. J Appl Polym Sci 1992, 46, 725.
31. Rokhade, A. P.; Patil, S. A.; Aminabhavi, T. M. Carbohydr Polym 2007, 67, 605.
32. Mundargi, R. C.; Shelke, N. B.; Rokhade, A. P.; Patil, S. A.; Aminabhavi, T. M. Carbohydr Polym 2008, 71, 42.